Electrochemical, Structural and Optical Studies on Poly(vinylidene chloride-co-acrylonitrile) Based Polymer Blend Membranes

C. Subbu[1,2], Chithra M. Mathew[1], K.Kesavan[1], S. Rajendran[1,*]

[1]School of Physics, Alagappa University, Karaikudi, Tamilnadu -630004, India.
[2]Alagappa Government Arts College, Karaikudi, Tamilnadu -630003, India.
[*]E-mail: sraj54@yahoo.com

Poly (ethylene oxide) (PEO), poly(vinylidene chloride -co-acrylonitrile) (PVdC-co-AN) and Lithium perchlorate ($LiClO_4$) based solid polymer blend electrolytes were prepared by solvent casting technique. The ionic conductivity of the polymer blend electrolytes was investigated by varying the PEO and PVdC-co-AN ratio. The maximum ionic conductivity was found to be 2.16×10^{-6} *Scm^{-1}* at 303*K* for PEO (80*wt%*)/PVdC-co-AN(20*wt%*)/$LiClO_4$ (8*wt%*). The structural studies were carried out by X-ray diffraction analysis. The complex formation between the polymers and the salt was confirmed by FT-IR study. The thermal properties of the samples were examined by DSC and TG/DTA. Surface morphology and topographical images of the sample having a maximum ionic conductivity were scrutinised by SEM and AFM respectively. The photoluminescence spectra show the correlation with the conductivity. The direct and indirect band gap energies were calculated by UV- visible studies.

Keywords: Polymer electrolyte; Poly (ethylene oxide) (PEO); poly(vinylidene chloride-co-acrylonitrile) (PVdC-co-AN); Optical band gap; Glass transition temperature.

1. INTRODUCTION

The solid polymer electrolytes (SPE) are considered as a potentially safer alternative for liquid electrolytes in lithium ion batteries because liquid electrolytes are easily subjected to exothermic decomposition resulting in thermal run away and an explosion [1-3]. In addition, the SPEs are less flammable and resistive to lithium dendrites formation; for this reason they have received considerable attention and have been extensively investigated for advanced electrochemical applications such as high energy density batteries, electrochromic displays and windows, sensors, fuel cells etc. Despite their advantages in safety, SPEs are challenged by the low ionic conductivity. As poly (ethylene oxide)

PEO has the chemical stability, electrochemical stability and capable of solvating a variety of alkali metal salts, it has been widely explored [4-11]. Lithium ions coordinate with the ether oxygen groups when the Lithium salt is dissolved in a PEO matrix. These Li^+ ions contribute to the ion conduction through the segmental motion of the polymer chains. In most of the cases, PEO based electrolytes have a high degree of crystallization and offer very low ionic conductivity at room temperature $\sigma = 10^{-8}-10^{-7}$ *Scm^{-1}* for $LiClO_4$−PEO [12]. Many research attempts have been made to minimise the crystalline nature of PEO. Blending is one of such technique that completely redefines the physical and chemical properties of PEO [13, 14]. In this present work poly(vinylidene chloride-co-acrylonitrile) (PVdC-co-AN) has been chosen as the other polymer to blend with PEO. For as PVdC-co-AN is concerned, it has been used very little in the field of polymer electrolyte, and its mechanical and thermal stabilities are superior to PEO. Barring that, it can modify the room temperature conductivity of PEO [15]. The present work reports the study on PVdC-co-AN/PEO polymer electrolyte membranes. The electrochemical, morphological, structural, functional, and thermal properties were evaluated.

2. EXPERIMENTAL AND CHARACTERIZATION TECHNIQUES

The polymers poly (ethylene oxide) (PEO; average $M_w \sim 8000$), poly(vinylidene chloride-co-acrylonitrile) (PVdC-co-AN; average $M_w \sim 150,000$) and salt $LiClO_4$ were purchased from Sigma Aldrich, USA. The polymers and salts were separately allowed to dissolve in the organic solvent Tetrahydrofuran (THF; Merck). Then, they were poured into a conical flask and stirred for $24h$ with a magnetic stirrer in order to get a homogeneous solution. The highly viscous homogeneous solution was poured onto well-cleaned glass plates after the air bubbles were removed. The residual solvent in the solution was removed by placing the glass plates in a vacuum oven for $12h$ at a temperature of 50 °C. At last, the polymer electrolyte films were gently removed from the glass plates and cut into desired dimensions. Then they were preserved in evacuated desiccators. In our experiments, typically four types of blend membranes with PEO weight percentage (*wt.%*) of 40, 50, 60, and 80 are prepared and denoted as SA1, SA2, SA3, and SA4.

The obtained electrolyte membranes were subjected to various analytical techniques. The blended electrolytes were structurally characterized at room temperature by X-ray diffraction analysis using X'pert PRO PANalytical X-ray diffractometer. The complex formation was ascertained from FT-IR using SPECTRA RXI, Perkin Elmer spectrophotometer in the range 400−4000 *cm^{-1}*. The impedance studies were carried out by sandwiching the polymer film between the stainless-steel blocking electrodes using a computer controlled micro Autolab type III Potentiostat/Galvanostat in the frequency range $100Hz-300KHz$. Thermal stability of the prepared blend was characterized by PYRIS DIAMOND TG/DTA analyser from room temperature to $750°C$ with the scan rate of $10°C$ min^{-1}. The change in glass transition temperature of the prepared films was done by differential scanning calorimeter using Mettler Toledo DSC (822e). The photoluminescence studies were performed by Carry Eclipse Fluorescence Spectrometer. UV-visible analysis was used to calculate the optical band gap of the electrolytes by (Lambda 35) Perkin Elmer UV-Visible spectrometer. The surface

morphology of the sample having a maximum ionic conductivity was analysed by JEOL, JSM-840A scanning electron microscope and its topographic images were scanned by AFM (A100SGS).

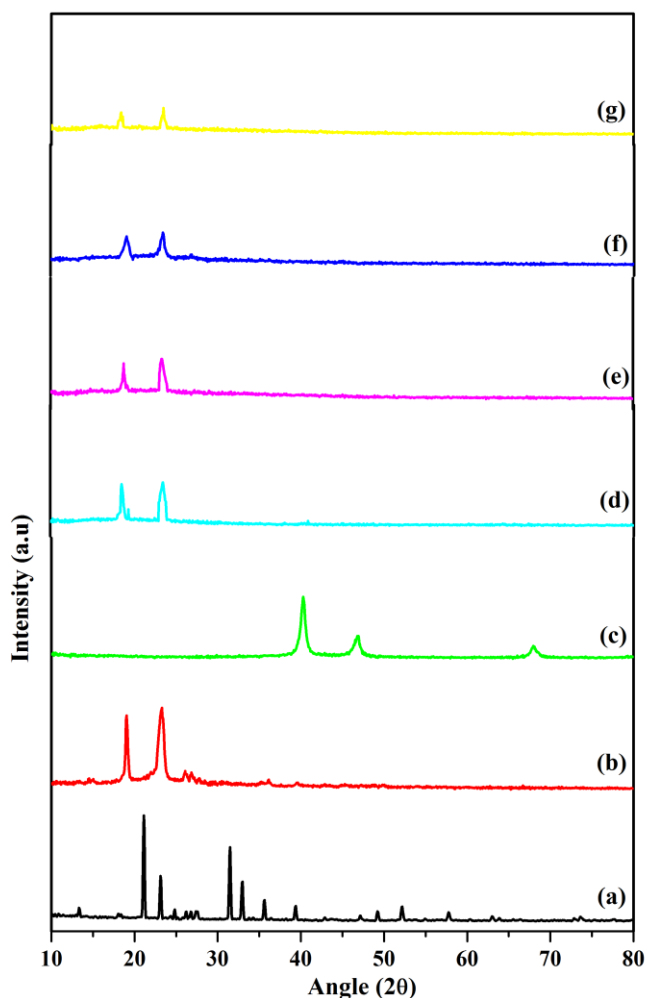## 3. RESULTS AND DISCUSSION

3.1 Structural Analysis

Figure 1. XRD patterns of (a) pure LiClO$_4$; (b) pure PEO; (c) pure PVdC-co-AN; (d) SA1; (e) SA2; (f) SA3: (g) SA4.

The X-ray diffraction analysis is a non-destructive analytical technique that gives the information about the crystallographic structure, chemical composition, and physical properties of materials and thin films, was performed to examine the structural changes in the prepared polymer blend films. The X-ray diffraction patterns of the pure and prepared complexes are shown in figure 1. From the figure 1(a), we can observe intense peaks at angles 2θ = 20.9, 22.92, 26.56, 32.75 and 35.4°

for pure LiClO$_4$ salt which show the crystalline nature. The peaks at 2θ = 19.1 and 23.3° in figure 1(b) indicate the semi crystalline nature make-up of pure PEO. Three diffraction peaks were observed at 2θ = 40.25, 46.6 and 67.9° for PVdC-co-AN which are due to the crystalline state of the polymer. It is found that there is a gradual decrease in the relative intensity of the characteristic peaks in the complexes when PEO ratio was increased as shown in figure 1(d-g). The diffraction peaks become weaker and broader when LiClO$_4$ salt is introduced in the complexes, suggesting the interaction between ether oxygen atoms of PEO and Li$^+$ [16]. The disappearance of high intense peaks of LiClO$_4$ confirms the maximum dissolution of the salt in the polymer matrix. In addition, there is no much change in PEO peak position. Hence, it can suggest that the polymer undergoes significant structural reorganization while blending and thus complexation occurs in the amorphous phase. It has been reported that ions are favourably mobile in the amorphous phase since their motion is assisted by polymer segmental motion [17].
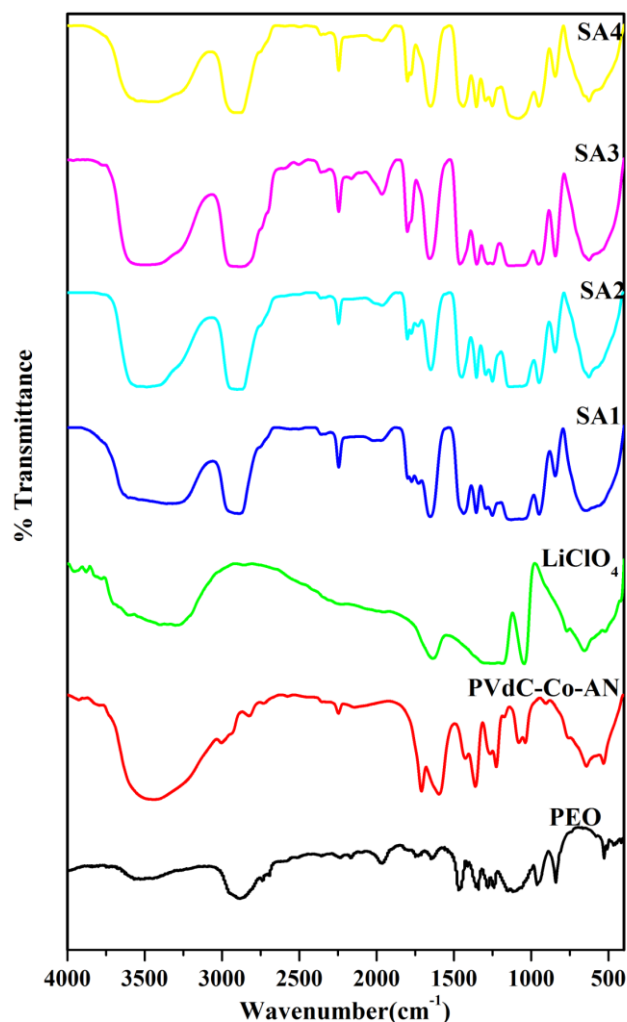
3.2 FT-IR analysis

Figure 2. FT-IR spectra of the pure and prepared samples.

On blending two polymers with the addition of salt, the cation of the metal is expected to coordinate with the polar groups in the host polymer matrix, resulting in complexation. This type of interaction will influence the local structure of the polymer segments and certain infrared active modes of vibration will be affected [18]. In such circumstances, the infrared spectroscopic studies will give the evidence of the complexation. The FT-IR spectra of pure PEO, PVdC-co-AN, LiClO$_4$ and the blends are given in figure 2.

The strong peaks around 2245 and 1642 cm^{-1} are attributed to the stretching vibrations of the nitrile groups C≡N and C=N in PVdC-co-AN [19]. The peak at 1799 cm^{-1} is the characteristic of the ether oxygen group stretching vibration in PEO [20] which is found shifted to 1743 cm^{-1}. The strong peak at 1100 cm^{-1} has been shifted to 1116 cm^{-1} which is assigned to the anti-symmetric stretching vibration of C−O−C bridge present in PEO [21]. The symmetric twisting mode observed at 1242 cm^{-1} in all complexes corresponds to the −CH$_2$ in PEO [20]. The −CH$_2$ asymmetric wagging in PEO is attributed to the peak around 1360 cm^{-1} [22]. The appearance of the peak at 845 cm^{-1} may be ascribed to the −CH$_2$ rocking mode in PEO [23]. The peak observed at 625 cm^{-1} in the polymer blend films is identified as the coordinated ClO$_4^-$ ion vibration [24]. The broad vibrational band around 3445 cm^{-1} in the spectrum corresponds to –OH group in PEO.

Table 1. Assignments of FT-IR absorption bands for prepared membranes.

Band assignment	Wavenumber cm^{-1}					
	PEO	PVdC-co-AN	SA1	SA2	SA3	SA4
−CH$_2$ Sym Stretching	2884		2880	2901	2911	2878
C≡N Stretching	-	2245	2245	2246	2245	2245
C=O Stretching	1743	-	-	1774	1776	1772
C=N Stretching	-	1642	1657	1650	1650	1659
−CH$_2$ Wagging	1360	-	1351	1354	1350	1356
−CH$_2$ Twisting	1242	-	1249	1250	1246	1252
C−O−C	1116	-	1140	1139	1106	1100
CH$_2$−CH$_2$	962		951	949	953	934
−CH$_2$ rocking	845	-	843	845	844	850
ClO$_4^-$	-	-	626	626	625	634

Table 1 shows the vibrational assignments of polymer blend films. The shift in the peaks, appearance, and disappearance of new peaks strongly affirms the complex formation.
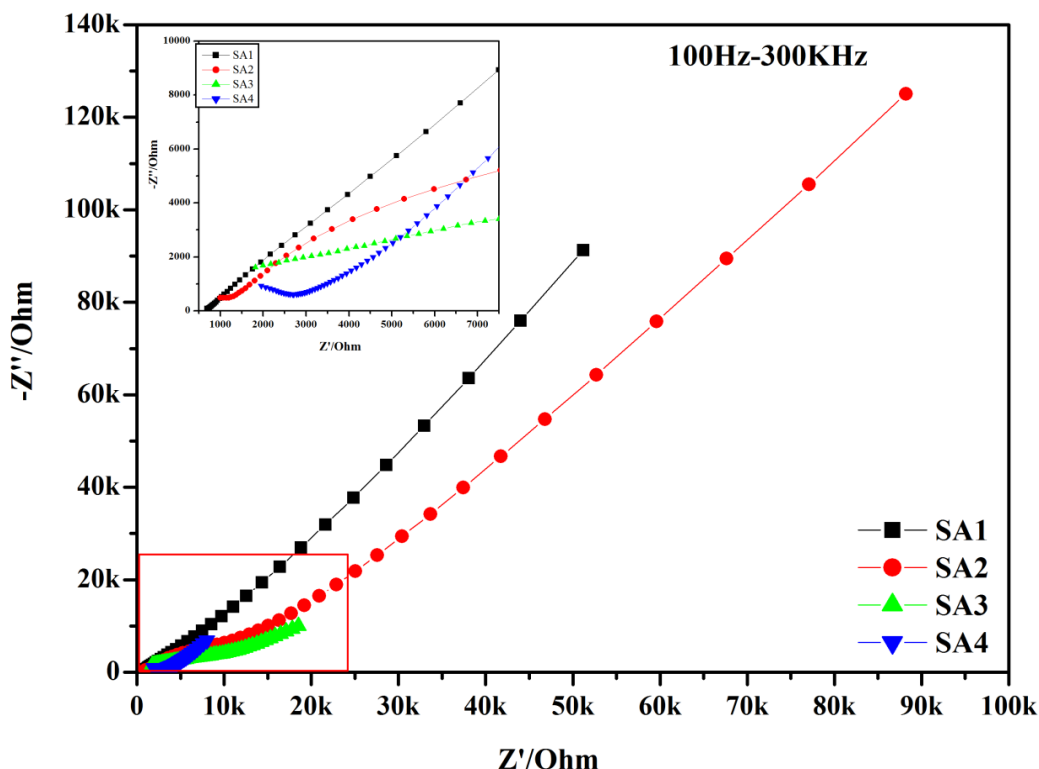
3.3 Impedance Analysis

Figure 3. Room temperature complex impedance plots of the prepared complexes.

The electrochemical impedance spectroscopy (EIS) is an effective and an excellent tool for studying the ionic conductivity of the polymer electrolytes. The complex impedance plots for the prepared samples at room temperature are given in figure 3. The absence of a high frequency semicircular portion in the figure shows that, the current carriers due to ions are responsible for the total conductivity [25]. The low frequency region of the curve should be a straight line, which is parallel to the imaginary axis in ideal condition, but it appears curved because of the double layer blocking electrodes [26]. The ionic conductivity was calculated using the relation $\sigma = l/R_b A$, where *l* is the thickness of the film, *A* is the area of the film and R_b bulk resistance of the polymer film. The R_b value is obtained from the high frequency intercept on X-axis. It is visualised from the plot that when PEO ratio increases from 40 to 80 *wt%* the bulk resistance values decrease. This may be due to the increase in ionic mobility and enhancement of the polymer segmental motion [27]. The conductivity values calculated for the prepared samples are listed in the Table 2. From the table it is observed that the maximum ionic conductivity value was found to be 2.6×10^{-6} *Scm*$^{-1}$ for the ratio PEO (80*wt%*)/PVdC-co-AN(20*wt%*)/LiClO$_4$(8*wt%*).

Table 2. Ionic conductivity values of the prepared samples.

Sample code	Composition of the prepared samples in wt%			Conductivity values for different temperatures $(\sigma) \times 10^{-6}$ Scm^{-1}					
	PVdC-co-AN	PEO	LiClO$_4$	303K	313K	323K	333K	343K	353K
SA1	60	40	8	0.64	1.20	2.33	3.98	6.17	8.53
SA2	50	50	8	0.77	1.54	2.45	4.27	6.76	9.94
SA3	40	60	8	1.40	2.03	3.33	5.32	7.6	11.5
SA4	20	80	8	2.16	3.11	5.47	7.05	9.87	16.4

From the table it is observed that the maximum ionic conductivity value was found to be 2.6×10^{-6} Scm^{-1} for the ratio PEO (80$wt\%$)/PVdC-co-AN(20$wt\%$)/LiClO$_4$(8$wt\%$).
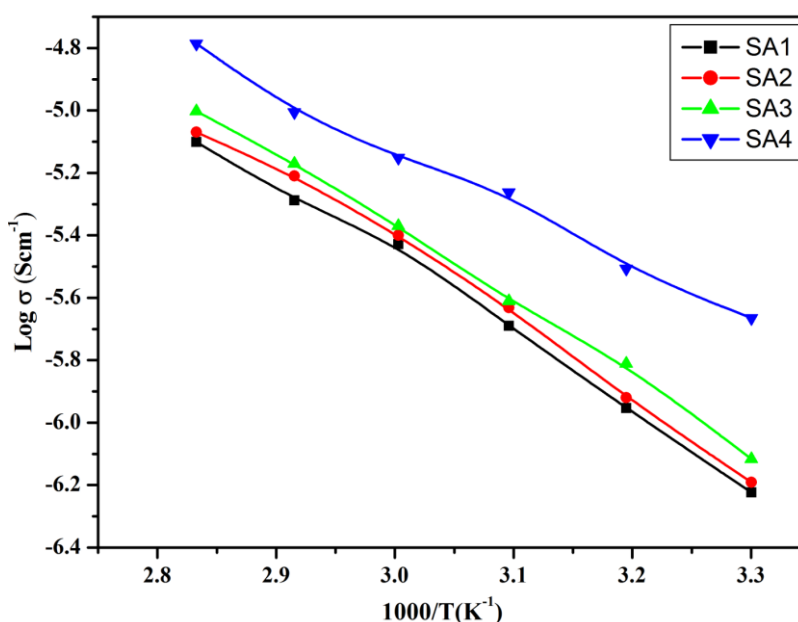

Figure 4. Temperature dependent ionic conductivity plots of the prepared samples.

The temperature dependent ionic conductivity plots of the prepared samples are shown in figure 4. From the plots, it can be understood that the ionic conductivity increases with increase in temperature over a range of 303K to 363K as shown in Table 2. This is due to the volumetric change. The increase in free space or the volume with respect to temperature is in accordance with the free volume theory, which paves the way for the easy movements of the polymer segments and ions. According to this free volume theory, the movements of the polymer chain segments and the dissociation of ions from the salt are improved when it is heated, and results in increased ionic conductivity at elevated temperature. The lithium salts tend to salt-polymer or cation-dipole interactions and thereby exists the cohesive energy at low temperature. This cohesive energy retards the quick movement of the polymer segments and the ions and hence the conductivity is lower at lower

temperature. The non-linearity observed in the plots indicates that the ionic conductivity obeys the Volgel-Tamman-Fulcher (VTF) relation $\sigma = AT^{-1/2} \exp\left(-B/(T - T_o) \right)$

where A is proportional to the number of charge carriers, T_o is the temperature of zero conductance and B is the activation energy. The VTF dependence is characteristic of an amorphous material above the glass transition temperature; which shows the flexibility of the polymer chains. The complexation occurred on blending is already observed in diffraction patterns. Hence, the obtained result clearly reveals that the segmental motions of the polymer-salt complex control the ion conduction significantly in polymer electrolytes.

3.4 Thermal analysis

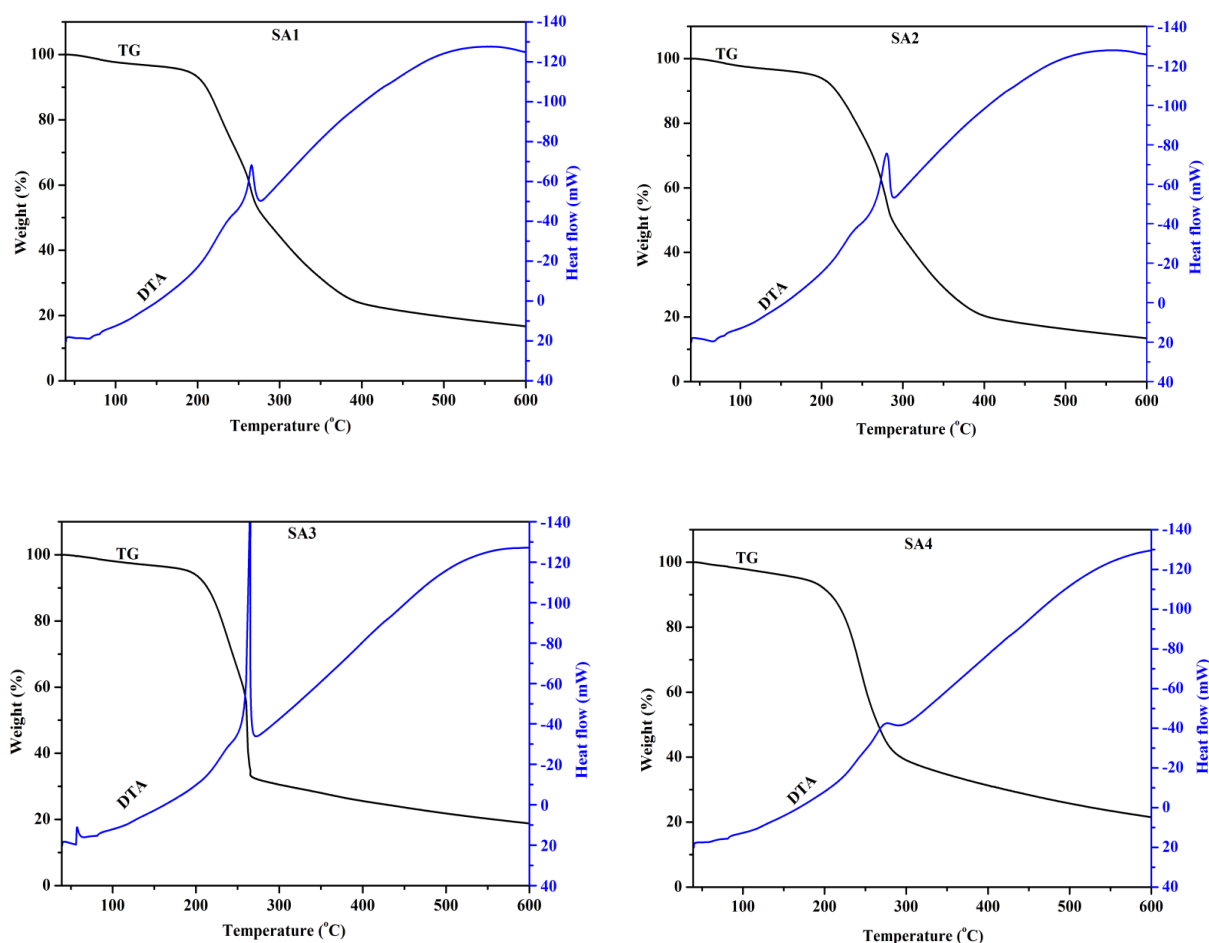### 3.4.1 Thermogravimetric Analysis

Figure 5(a-d). TG/DTA plots of the prepared blend electrolytes.

In order to investigate the thermal stability of the prepared samples, the prepared films were subjected to TG/DTA analysis. The TG/DTA curves of the prepared blends are shown in figure 5 and the results have been listed in the table 3.

Table 3. TG/DTA results of the prepared samples.

Sample code	Decomposition temperature (^{0}C)			weight loss of the samples in %			Exothermic peaks (^{0}C)		
	I	II	III	I	II	III	I	II	III
SA1	71	268	401	2	46	77	68	265	-
SA2	82	284	397	2	50	80	68	279	-
SA3	90	260	267	2	44	67	58	264	-
SA4	75	271	309	1	54	61	74	277	-

From the figure, it is obvious that the initial weight loss takes place around 71−90 °C that is about 1-2 %. This may be due to the removal of the residual solvents and moisture. The second weight losses 46, 50, 44, and 54 % corresponding to the temperatures 268, 284, 260 and 271°C were observed for the samples SA1, SA2, SA3, and SA4 respectively. This may be due to the structural change in the polymer blends. The samples exhibit decomposition in the temperature range 267−401°C. The thermal stability of the samples SA1, SA2, SA3, and SA4 are 185, 200, 192, and 181 °C respectively. The DTA curves of the sample showed exothermic peaks from 264 to 277 °C due to melting of prepared films, which are well correlated, with the weight loss of the samples in TGA. The maximum thermal stability 200°C is observed for the sample SA2 (PEO/PVdC-co-AN; 50:50 *wt%*). Nevertheless, the sample SA4 (80:20 *wt%*) exhibits maximum ionic conductivity.

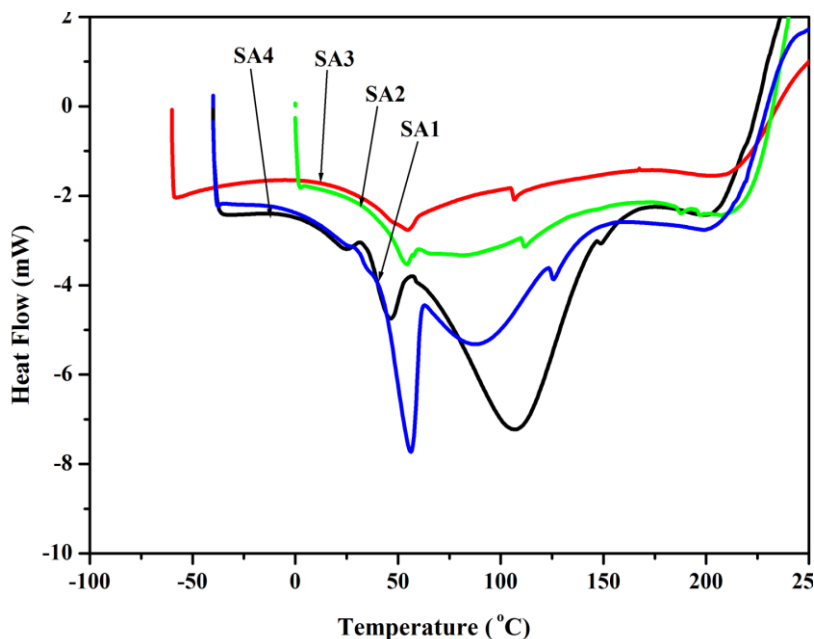*3.4.2 Differential scanning calorimetric Analysis*

Figure 6. DSC curves of prepared polymer electrolytes.

The DSC curves of the polymer electrolytes with different PEO/PVdC-co-AN ratios are as shown in figure 6. Since the T_g of PEO is -53 to -45 °C and that of PVdC-co-AN is about 50°C, the prepared blends show a phase transition from 33 to 42 °C. This is attributed to the glass transition temperature of the samples and the T_g value is found to be decreased with the addition of PEO to the copolymer PVdC-co-AN. The minimum value of T_g = 33°C is observed in the sample having a blend ratio PEO/PVdC-co-AN (80:20) *wt%*. The decrease of T_g enhances the segmental mobility which in turn may assist to improve the ionic conductivity. Thus, DSC analysis gives a good agreement with impedance result. The secondary peak indicates the melting point of the blends that varies from 281 to 285 °C.

3.5 Morphological Analysis

3.5.1 Scanning electron microscopic Image

The scanning electron microscope is an excellent tool to study the surface morphology of the sample. The scanning electron micrograph of PEO/PVdC-co-AN complex having maximum ionic conductivity (blend ratio 80:20) is given in figure 7. The morphological images of the film with two different magnifications (1*K* and 10*K*) show the presence of the tails like interconnected polymer chains and maximum number of micro pores [28]. The pores are formed due to the evaporation of solvent from the membrane and the presence of these pores is responsible for entrapping large volumes of the liquid in the cavities. In addition, the surface morphology reveals that there is no separate phase formed between PEO and PVdC-co-AN which reveals the miscibility as observed in XRD pattern.
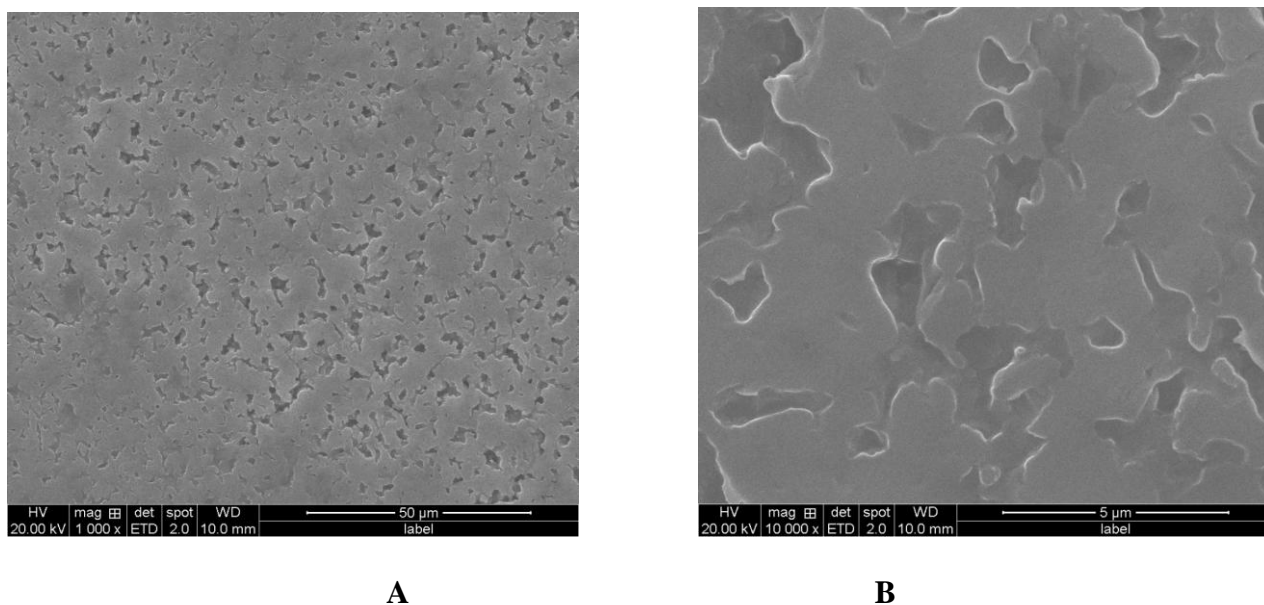

A **B**

Figure 7. SEM analysis of the sample (SA4) having maximum ionic conductivity at different magnifications. (a)1000X; (b) 10000X.

3.5.2 Atomic Force Microscopic Image

The blend polymer film having a maximum ionic conductivity-SA4 (blend ratio 80:20) was subjected to atomic force microscope analysis that is used to study the two and three-dimensional topographical images of the film.
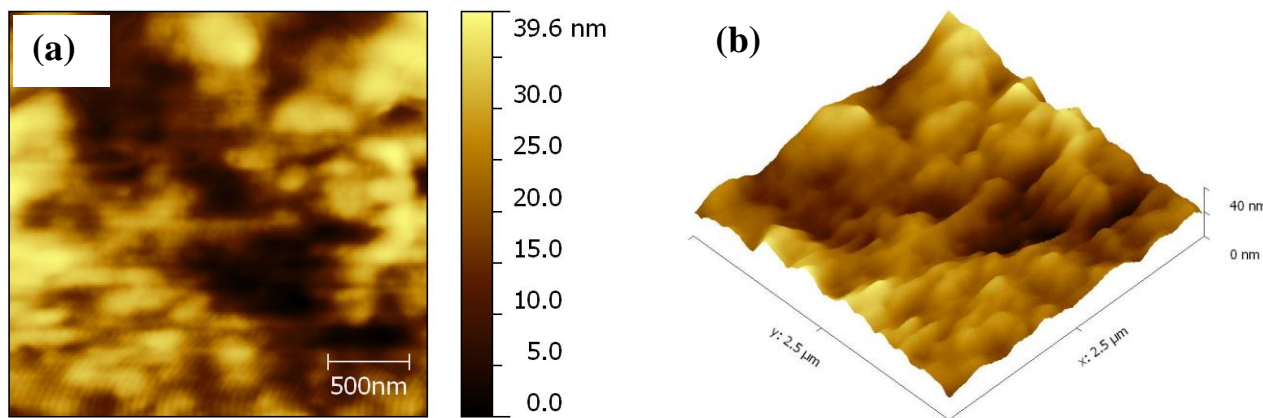

Figure 8. (a) Two-dimensional AFM image of the sample SA4, **(b)** Three-dimensional AFM image of the sample SA4.

The figure 8(a&b) shows the two and three-dimensional images. It is noted that there are a large number of pores of size 40 *nm* within the scanned area of 2.5*μm*×2.5*μm* and the root means square roughness of the film is found to be 52 *nm* [29]. The length of the segmental chain is 500 *nm*. Thus, the presence of maximum number of pores favours the ionic conductivity.

3.6 Optical Analysis
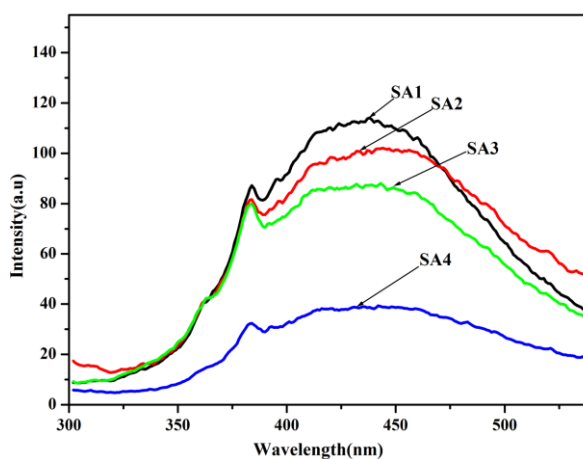
3.6.1 Photoluminescence Spectra

Figure 9. Photoluminescence spectra of the prepared complexes.

The photoluminescence studies were carried out for all the blended films at an excitation wavelength of 280 *nm* as shown in the figure 9 and the corresponding emission spectra was obtained around 380 *nm*. From the figure, it is clear that the film with PEO (80*wt%*)/PVdC-co-AN(20*wt%*)/LiClO$_4$(8*wt%*) shows minimum fluorescence emission intensity. It was reported that the fluorescence intensity is inversely proportional to the local free volume and directly proportional to the local viscosity of the electrolyte medium [30]. Since the blend ratio (80:20) shows minimum fluorescence intensity, it is expected that the film contains large free volume and hence low viscosity. Because the ionic conductivity is directly associated with the local free volume, fluorescence spectra reveals that the sample shows minimum intensity which gives maximum ionic conductivity. Thus, photoluminescence study strongly ascertains the maximum ionic conductivity of the sample SA4 [31].

3.6.2 UV-Vis Spectra

The optical band gap of the polymer electrolytes was determined using UV-Visible spectra. The optical absorption of the solids gives its band structure. Semiconductors are generally classified into two types (a) direct band gap (b) indirect band gap. The band gap is said to be direct band gap when the top of the valence band and the bottom of the conduction band have the same zero crystal momentum (wave vector). In addition, it is said to be indirect band gap when the bottom of the conduction band does not correspond to zero crystal momentum.
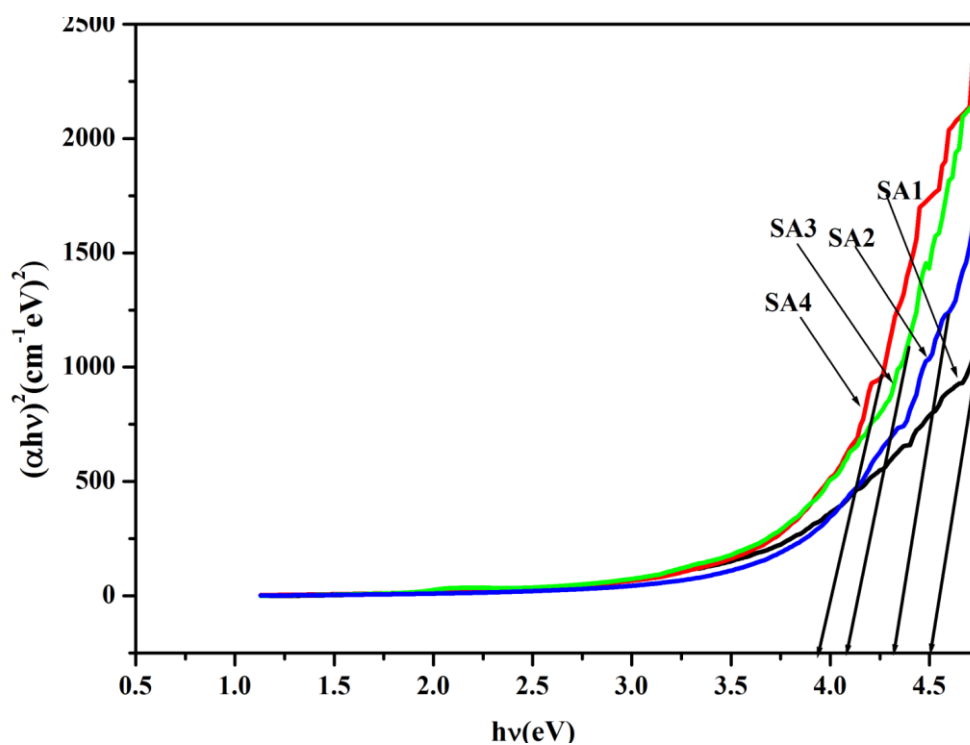

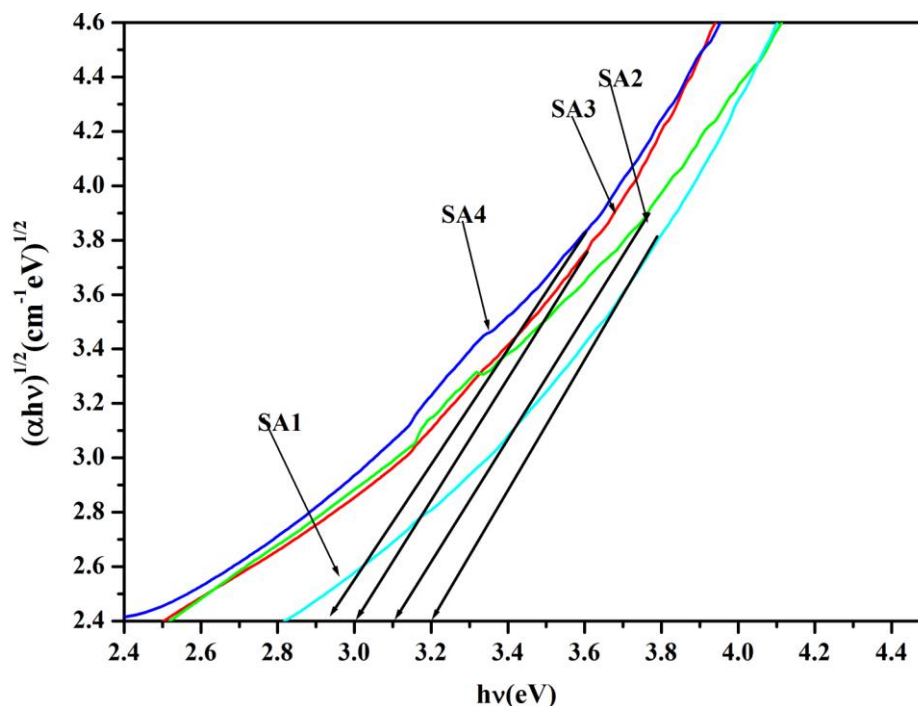**Figure 10.** Plots for direct band gap of the prepared samples.

Figure 11. Plots for indirect band gap of the prepared samples.

The transition from valence band to conduction band should always be associated with a phonon in indirect band gap materials. The fundamental absorption corresponding to the transition from valence band to conduction band is used to determine band-gap of the materials. The relation between the absorption co-efficient (α) and incident photon of energy ($h\nu$) can be written as [32]

$$\alpha = C\left[\frac{(h\nu - E_g)^n}{h\nu}\right]$$

where C is a constant and E_g is the band gap of the material. The exponent n depends on the type of transition and it takes the values ½ for direct, 2 for indirect and for forbidden direct and forbidden indirect transitions respectively.

Figure 10 and figure 11 show the plots of the prepared complexes with $(\alpha h\nu)^2$ and $(\alpha h\nu)^{1/2}$ as functions of $h\nu$ for direct and indirect transitions respectively. It is found from the plot that the band gap of the complexes goes on decreasing from 4.5.to 3.9 in the direct band gap calculation and from 3.2 to 2.9 in the indirect band gap calculation. The decrease in the band gap shows the compositional change in the host materials [33, 34]. The reported band gap value of the pure PEO/PVdC-co-AN is found greater than that of the prepared complexes. The film with (80:20) blend ratio, SA4 in both plot exhibits least band gap energy whose conductivity is found to be the highest.

4. CONCLUSIONS

The polymer electrolytes based on fibrous PEO/PVdC-co-AN blend membranes are prepared by solution casting technique. The thermal stability is found higher for the polymer blends comprising

50:50 *wt.%* composition. The crystallinity of the polymer blends is studied by DSC and XRD and the results show that the component polymers in the blends are miscible. It is worth to mention that, the ionic conductivity is improved by increasing PEO content. Among the polymer electrolytes prepared, the maximum ionic conductivity is 2.16×10^{-6} *Scm^{-1}* at 303*K*. The optical and morphological analyses of the films are in good agreement with impedance analysis and can be used in lithium battery application.

References

1. P. G. Balakrishnan, R. Ramesh and T.P. Kumar, *J. Power source,* 155 (2006) 401
2. Z. Zhang, D. Fouchard and J.R. Rea, *J. Power source,* 70 (1998) 16
3. K. Xu, *Chem.Rev.,* 104 (2004) 4303
4. D.E. Fenton, J.M. Parker and P.V. Wright, *Polymer,* 14 (1973) 589
5. MB. Armand, *Solid State Ionics,* 69 (1994) 309
6. J.R.MacCallum and C.A. Vincent, (Eds) *Polymer Electrolyte Review-1*, Elsevier Applied science, New York (1987)
7. F. Grey, *Solid polymer Electrolytes*; VCH Publishers: New York (1991)
8. W.H. Meyer, *Adv.Mater*., 10 (1998) 439
9. R.C. Agarwal and G.P. Pandey, *J. Phys. D: Appl. Phys,* 41 (2008) 223001
10. A.M .Stephen and K.S. Nahm, *Polymer*, 47 (2006) 5952
11. P.G.Bruce and C.A. Vincent, *J. Chem. Soc., Faraday Trans*, 89 (1993) 3187
12. C.D. Robitaille and D.J.Fauteux, *Electrochem. Soc*, 133 (1986) 315
13. K. Kiran Kumar, M. Ravi, Y. Pavani, S. Bhavani, A.K. Sharma, and V.V.R. Narasimha Rao, *Physica B*, 406 (2011) 1706
14. S. Ramesh, Tan Winie, A.K. Arof, *Europ Polym J*., 43 (2007) 1963
15. M. Shanthi, C. M. Mathew, M. Ulaganathan and S. Rajendran, *Spectrochim. Acta Part A,* 109 (2013) 104
16. Jingyu Xi and Xiaozhen Tang, *Chem. Phys. Letters,* 393 (2004) 271
17. J.L. Souquet, *Ann Rev Mater Sci.,* 11 (1981) 211
18. Polymer Blends and Alloys (Eds) Gabriel O. Shonaike and George P. Simon, Marcel Dekker, USA (1999)
19. S. Krimm and C.Y. Liang, *J. Polym. Sci*., 22 (1956) 95
20. B. L. Papke, M. A. Ratner and D. F. Shriver, *J. Electrochem. Soc*., 129(7) (1982) 1434
21. S.J. Wen, T.J. Richardson, D.I. Ghantous, K.A. Striebel, P.N. Ross and E.J. Cairns, *J. Electroanalytical Chem,*. 408 (1996) 113
22. S.Austin Suthanthiraraj and D.Joice sheeba, *Ionics,* 13 (2007) 447
23. S.A.M.Noor, A.Ahamed, I.A.Talib and M.Y.A.Rahman, *Ionics,* 16 (2010)161
24. K. Kulasekarapandian, S. Jayanthi, A. Muthukumari, A. Arulsankar and B. Sundaresan, *Int. J. Eng. Res. Develop.,* 5 (2013) 30
25. S.Izuch, S.Ochiai and K.Takeuchi, *J. Power Source*, 68 (1987) 37
26. C.Kim, G.Lee, K. Lio, K.S.Ryu, S.G.Kang and S.H.Chang, *Solid state Ionics,* 123 (1999) 251
27. M. Jaipal Reddy, CH. Ramesh , J. Siva Kumar and U.V. Subba Rao, *Int. J. Appl. Eng. Res,* 2 (2011) 147

28. Li Jian, Xi Jingyu, SONG Qins and TANG Xiaozhen, *Chinese Sci. Bull.,* 50 (2005) 368
29. I. Horcas, R. Fernandez, J.M.G. Rodriguez, J. Colchero, J.G. Herrero and A.M. Baro, *Rev. Sci. Instrum,* 78 (2007) 013705
30. U.S. Park, Y.J. Hong, and S.M. Oh, *Electrochim. Acta,* 41 (1996) 849
31. V. Aravindan, P. Vickraman, and T.Prem Kumar, *J. Non-Cryst. Solids,* 354 (2008) 3451
32. S. Ibrahim, R. Ahmed and M. R. Johanl, *J. luminescence,* 132 (2012) 147
33. I. Sharma, S.K. Tripathi and P.B. Barman, *Appl. Surface Sci.*, 255 (2008) 2791
34. M. Kitao, H. Akao, T. Ishikawa and S. Yamada, *Physica Status Solidi (a)*, 64 (1981) 493